analytical chemistry

Article

Cite This: *Anal. Chem.* 2019, 91, 5433−5445

pubs.acs.org/ac

Site-Specific Glycosylation Quantitation of 50 Serum Glycoproteins Enhanced by Predictive Glycopeptidomics for Improved Disease Biomarker Discovery

Qiongyu Li,[†] Muchena J. Kailemia,[†] Alexander A. Merleev,[‡] Gege Xu,[§] Daniel Serie,[§] Lieza M. Danan,[§] Fawaz G. Haj,[⊥,∥] Emanual Maverakis,[‡] and Carlito B. Lebrilla*[,†]

[†]Department of Chemistry, University of California, One Shields Avenue, Davis, California 95616, United States

[‡]Department of Dermatology, University of California Davis, School of Medicine, Sacramento, California 95817, United States

[§]Venn Biosciences Corporation, 800 Chesapeake Dr., Redwood City, California 94063, United States

[⊥]Department of Nutrition, University of California, One Shields Avenue, Davis, California 95616, United States

[∥]Department of Internal Medicine, Division of Endocrinology, Diabetes, and Metabolism, University of California Davis, Sacramento, California 95817, United States

Supporting Information

ABSTRACT: Analysis of serum protein glycovariants has the potential to identify new biomarkers of human disease. However, the inability to rapidly quantify glycans in a site-specific fashion remains the major barrier to applying such biomarkers clinically. Advancements in sample preparation and glycopeptide quantification are thus needed to better bridge glycoscience with biomarker discovery research. We present here the successful utilization of several sample preparation techniques, including multienzyme digestion and glycopeptide enrichment, to increase the repertoire of glycopeptides that can be generated from serum glycoproteins. These techniques combined with glycopeptide retention time prediction and UHPLC-QqQ conditions optimization were then used to develop a dynamic multiple-reaction monitoring (dMRM)-based strategy to simultaneously monitor over 100 glycosylation sites across 50 serum glycoproteins. In total, the abundances of over 600 glycopeptides were simultaneously monitored, some of which were identified by utilizing theoretically predicted ion products and presumed m/z values. The dMRM method was found to have good sensitivity. In the targeted dMRM mode, the limit of quantitation (LOQ) of nine standard glycoproteins reached femtomole levels with dynamic ranges spanning 3−4 orders of magnitude. The dMRM-based strategy also showed high reproducibility with regards to both instrument and sample preparation performance. The high coverage of the serum glycoproteins that can be quantitated to the glycopeptide level makes this method especially suitable for the biomarker discovery from large sample sets. We predict that, in the near future, biomarkers, such as these, will be deployed clinically, especially in the fields of cancer and autoimmunity.

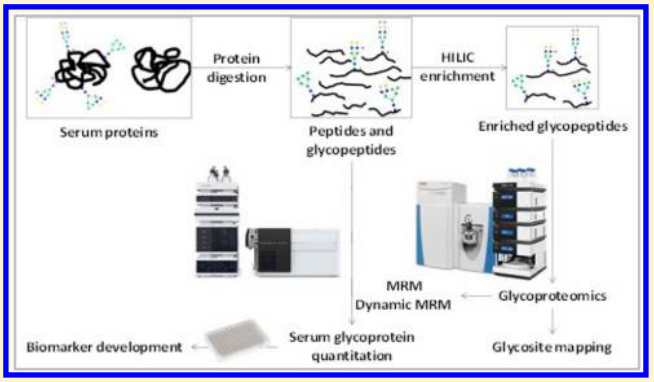

Single proteins in serum or plasma samples are widely used as biomarkers of human diseases. For example, the glycoprotein CA19-9 has been used as a sensitive biomarker for pancreatic cancer.[1] The discovery of new biomarkers, "indications of medical state observed from outside the patient—which can be measured accurately and reproducibly",[2] continues to be important for advancing disease diagnostics, drug development, and personalized medicine. In this setting, analysis of post-translational modifications (PTM), including phosphorylation, acetylation, glycosylation, and oxidation, may increase the specificity of existing biomarkers or lead to the discovery of new biomarkers with greater accuracy for detecting human diseases and predicting their outcomes or the likelihood that a patient will respond to therapy.[3]

Alterations in protein glycosylation have been known for decades to occur in patients with cancer and autoimmunity,[4,5] which is relevant because the majority of the United States Food and Drug Administration (FDA)-approved cancer biomarkers are glycoproteins, including CA 125 for ovarian cancer[6] and prostate-specific antigen (PSA) for prostate cancer.[7] However, analysis of their glycosylation is challenging because glycan structures are more complicated and heterogeneous compared to other PTMs. More than 70% of human blood proteins are glycosylated,[8] and they play outsized

Received: February 12, 2019
Accepted: March 14, 2019
Published: March 18, 2019

DOI: 10.1021/acs.analchem.9b00776
Anal. Chem. 2019, 91, 5433−5445

roles in cellular adhesion, communication, and metabolism. Only a few of these glycoproteins have been profiled in a glycan site-specific manner because site-specific glycan profiling remains a formidable challenge. Rather, current efforts toward glycan biomarker discovery typically focus on released glycans.[9] Analysis of released N-glycans from their attachment sites provides a global overview of the system-wide alterations in glycosylation, which has demonstrated some measure of success in biomarker research, as released glycans have been associated with a variety of diseases, including prostate[10] and ovarian[11] cancer.

In contrast to characterizing released glycans, analysis of protein-specific glycosylation combines both glycomic and proteomic information for biomarker discovery. However, current glycoproteomics methods require the depletion of the most-abundant serum proteins and the enrichment of glycoproteins.[12] Additionally, earlier studies have provided information on site occupation with no glycan information because degrading and releasing the N-glycan is central to most workflows.[13] Prior quantitation has also been limited to the glycoprotein level, using methods such as iTRAQ labeling, which mixes different biological samples and compares between specific states.[14]

A common method for multiplex quantitation in other fields employs a more targeted approach using an unique feature of mass spectrometry, the ability to monitor specific molecules based on their unique fragmentation. Multireaction monitoring (MRM) mass spectrometry is typically performed on a triple quadruple (QqQ) mass spectrometer and is widely used for analyte (including peptide) quantitation.[15] It has recently been used in this laboratory to quantify glycopeptides yielding both glycan and peptide specificity.[16,17] In the basic MRM method, masses are monitored along with their fragments throughout the chromatographic run. This method is highly analyte-specific and minimizes the issues associated with coeluting compounds, which may cause an ion suppression effect and hinder the identification of some lower abundance compounds.[18] In addition, the high selectivity of MRM allows better quantitation with high sensitivity compared to non-targeting proteomic methods.[19] However, monitoring analytes over the chromatographic period diminishes significantly the number of analytes that can be quantified. A more recent approach, termed dynamic MRM (dMRM), alleviates this limitation by monitoring analytes only at designated retention periods. A dMRM method was developed to comprehensively monitor with quantitation the glycopeptides from the four subclasses of immunoglobulin (Ig) G without enrichment.[16] It was further extended to 15 peptides together with 64 glycopeptides across IgG, IgA, and IgM.[17] With the defined retention time (RT) of each transition, more transitions can be monitored in a single run making it fast (15 min run), allowing it to be applied to large-size-sample-sets necessary for biomarker discovery.[20]

Herein, we have expanded the dMRM further to monitor 50 serum glycoproteins, which yielded nearly 700 unique glycopeptides and peptides using a targeted 50 min LC−MS run. The MRM is typically used for small analytes (less than 1 kDa), while glycopeptides can be as large as 5 kDa, requiring the diligent selection of targets with proper charge state. To determine the glycopeptides associated with each protein, an extensive site-specific glycan map of each protein was determined. Low abundant and potential glycopeptides that were expected but not observed in the initial library mapping effort were also monitored by generating virtual transitions and predicting the elution time of the predicted peptides. The RTs of these glycopeptides were predicted based on the hydrophobicities of their peptide backbones and the variation in RTs associated with the glycans. With these innovations, the coverage of the method reported herein is comparable to that of untargeted glycoproteomics methods but provides a much improved sensitivity and faster quantitation. The method was validated for quantitation and reproducibility by applying it to serum samples from 16 healthy adults. The linearity of protein and glycopeptide quantitation and the limit of quantitation (LOQ) were determined using standard proteins. This method is expected to find utility in large-sample-size studies for biomarker discovery where high throughput is important.

EXPERIMENTAL SECTION

Chemicals and Reagents. Glycoprotein standards purified from human serum/plasma were purchased from Sigma-Aldrich (St. Louis, MO). Peptide standards were purchased from A&A Laboratory (San Diego, CA). Sequencing grade trypsin and Glu-C were purchased from Promega (Madison, WI). Dithiothreitol (DTT) and iodoacetamide (IAA) were purchased from Sigma-Aldrich (St. Louis, MO). ISPE-HILIC cartridges were purchased from HILICON AB (Sweden). Human serum was purchased from Sigma-Aldrich (St. Louis, MO). Healthy serum samples were obtained from Dr. Haj's laboratory.

Sample Preparation. Serum samples and glycoprotein standards were reduced with DTT, alkylated with IAA, and then digested with trypsin in a water bath at 37 °C for 18 h. Two distinct procedures were followed for glycoproteomics and glycopeptide quantitation. For glycoproteomic analysis using LC−MS/MS, glycopeptides were enriched with iSPE-HILIC cartridges. To profile more glycosylation sites, serum samples were also digested with trypsin followed by Glu-C. For quantitation, tryptic digested samples were analyzed directly with no enrichment for glycopeptides. To determine the RT of glycopeptides in the liquid chromatography gradient, peptide standards were spiked in the serum sample and digested together to generate an RT standard curve for RT prediction.

LC−MS/MS Analysis. For the glycoproteomic analysis, enriched serum glycopeptides were analyzed with a Q Exactive Hybrid Quadrupole-Orbitrap Mass spectrometer. A C18 column and a 180 min gradient were used for glycopeptide separation. The solvents used were solvent A, composed of 3% of ACN, and solvent B, with 90% ACN in both aqueous solutions.

For quantitative analysis, tryptic-digested serum samples were injected into an Agilent 1290 infinity ultrahigh-pressure liquid chromatography (UHPLC) system coupled to an Agilent 6495 QqQ mass spectrometer. The separation was conducted on an Agilent Eclipse plus C18 (RRHD 1.8 μm, 2.1 mm × 150 mm) column coupled to an Agilent Eclipse plus C18 (RRHD 1.8 μm, 2.1 mm × 5 mm) guard column. Solvent A, containing 3% of ACN and 0.1% of FA and solvent B, containing 90% of ACN and 0.1% of FA both in water, were used for a 50 min binary gradient. The scan mode of the instrument used was dMRM.

Data Analysis. The tandem mass spectra (MS^2) collected from the Orbitrap were searched against the human proteome database and an in-house serum N-linked glycan library using the Byonic software (v3.0.0) (Protein Metrics, Inc.). The glycopeptides were identified based on their accurate masses

DOI: 10.1021/acs.analchem.9b00776
Anal. Chem. 2019, 91, 5433−5445

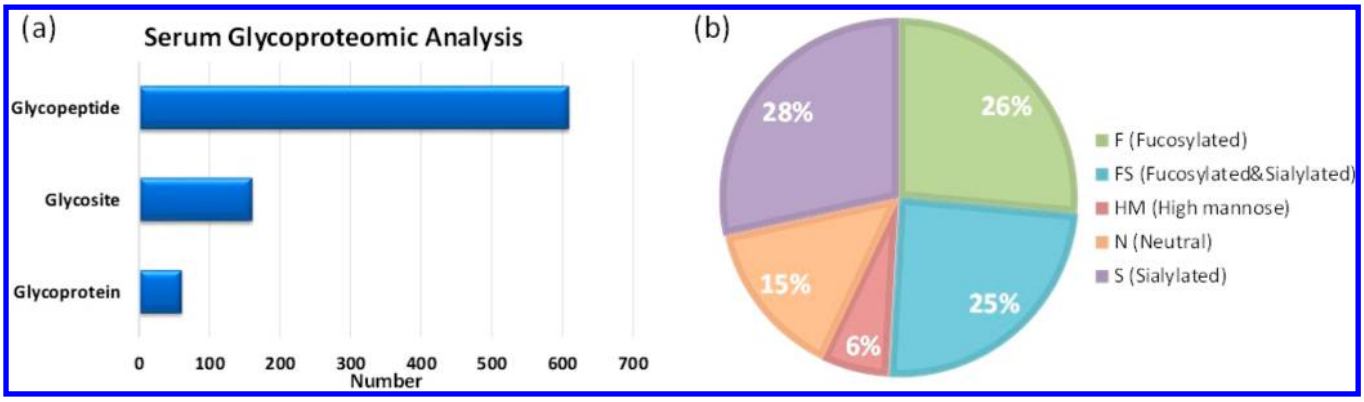

Figure 1. (a) The summary of serum glycoproteomic analysis showing the numbers of glycopeptides, glycosites, and glycoproteins. (b) Glycosylation types of serum glycoproteins.

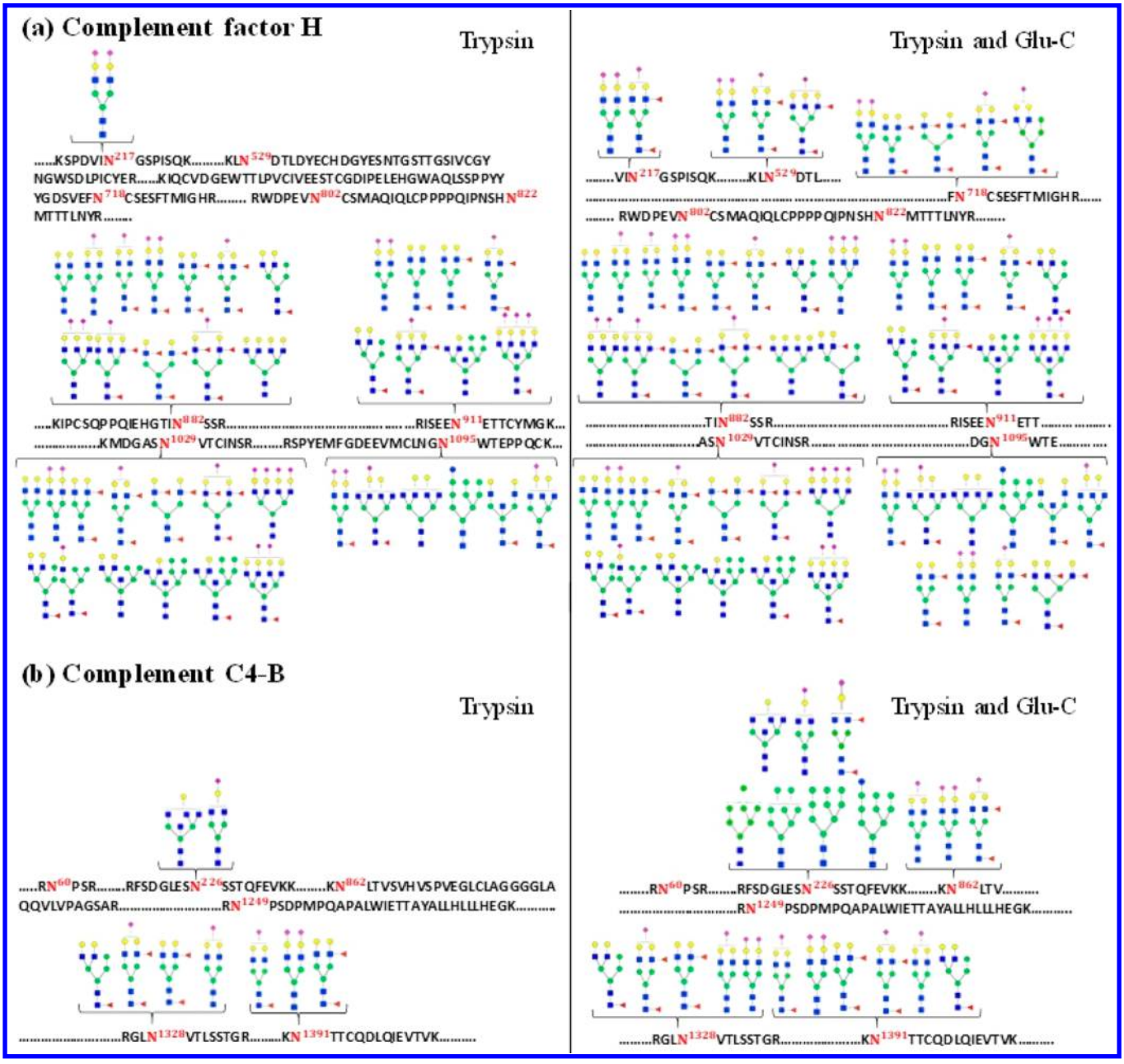

Figure 2. Glycosylation mapping using multiple-enzyme strategy of (a) complement component H and (b) complement C4B.

DOI: 10.1021/acs.analchem.9b00776
Anal. Chem. 2019, 91, 5433−5445

Table 1. Part of the MRM Transition List of Quantitative Peptides of Glycoproteins

protein	peptide	precursor ion	product ion
HEMO	NFPSPVDAAFR	610.8	959.5
HEMO	YYCFQGNQFLR	748.3	734.4
KNG1	YFIDFVAR	515.8	720.4
KNG1	YNSQNQSNNQFVLYR	625.6	550.3
CFAH	IDVHLVPDR	532.3	599.4
CFAH	SSQESYAHGTK	597.8	763.4
CO4B	VLSLAQEQVGGSPEK	771.4	373.2
CO4B	VTASDPLDTLGSEGALSPGGVASLLR	828.4	869.5
VTNC	FEDGVLDPDYPR	711.8	647.3
VTNC	DVWGIEGPIDAAFTR	823.9	1076.5
CO5	GIYGTISR	433.7	696.4
CO5	IPLDLVPK	447.8	781.5
ANGT	SLDFTELDVAAEK	719.4	316.2
ANGT	VLSALQAVQGLLVAQGR	862.0	431.2
ANT3	IEDGFSLK	454.7	666.3
ANT3	GDDITMVLILPKPEK	834.9	937.6
CFAI	IVIEYVDR	503.8	794.4
CFAI	VANYFDWISYHVGR	576.3	640.3

and fragment ions. The N-glycans and O-glycans produce unique fragments with m/z values of 204.08 for the hexosamine residue (HexNAc), 366.14 for the residue of one hexose and one hexosamine ($Hex_1HexNAc_1$), and 292.09 for the sialic acid residue (Neu5Ac). These oxonium ions generally yielded higher abundances than other fragment ions therefore they are used primarily for quantitation of glycopeptides. The Y1 ions also are often present but in significantly lower abundances. A 1% false discovery rate (FDR) was applied to limit the number of false positive identifications. The quality control of the database searching results wass done by filtering the glycopeptide compositions according to |Log Prob| (greater than 2) and Delta Mod (greater than 10) values.

The glycoproteomic data were used to develop the MRM method. The standard curve of RTs varying with the hydrophobicities of synthesized peptide standards was used to acquire the predicted RT of glycopeptides. Then, the RT of each glycopeptide was included in the MRM method for developing the dMRM method, which was used for simultaneous quantitation of glycopeptides and peptides. The dMRM data from QqQ was analyzed with Agilent MassHunter Quantitative Analysis B.5.0 software. Peak areas acquired from the software were used for quantitation. The linear range of protein quantitation was determined by evaluating the concentration range where the signal varies linearly with the concentration. A signal-to-noise ratio (S/N) of 6 was used to determine the limit of quantitation (LOQ), and 3 was used for the limit of detection (LOD). The statistical analyses, including PCA and the Pearson product-comment correlation coefficient (PPMCC), were also conducted to observe the correlations between different glycopeptides.

Table 2. Hydrophobicity Values and RTs of Peptide Standards

peptide	RT	hydrophobicity
RDNYTK	1.090	4.14
RDDYTK	1.092	5.49
DNNSIITR	7.487	15.92
DDNSIITR	7.515	17.60
ENETEIIK	8.626	17.54
EDETEIIK	8.636	19.21
WSDIWNATK	16.398	30.16
WSDIWDATK	16.437	33.52
YGNPNETQNNSTSWPVFK	17.327	31.02
YGNPNETQNDSTSWPVFK	17.337	32.50
PKNATVLIWIYGGGFQTGTSSLHVYDGK	28.040	47.33
PKDATVLIWIYGGGFQTGTSSLHVYDGK	28.084	48.57

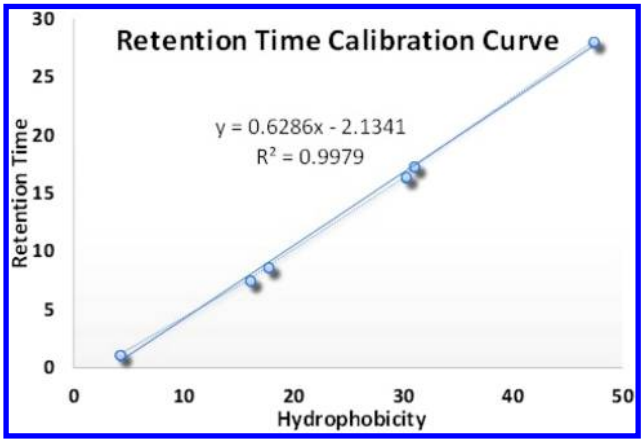

Figure 3. Calibration curve of RTs generated from peptide standards

RESULTS AND DISCUSSION

Construction of Glyco-Map for Human Serum. A site-specific glycomap of serum glycoproteins was constructed using commercial serum (Sigma-Aldrich). To overcome the suppression of signals by peptides and facilitate the detection of glycopeptides, HILIC cartridges were used to enrich glycopeptides. Enrichment is performed only during the mapping process because, for the quantitation of glycopeptides, the loss of some glycopeptides due to the enrichment will lead to poor reproducibility. Analysis of the serum sample using the Byonic software (Protein Metrics) yielded over 600 glycopeptides corresponding to 69 unique glycoproteins and 160 glycosylation sites (Figure 1a). Among the glycopeptides, 26% were only fucosylated, 28% were only sialylated, and 25% were both fucosylated and sialylated (Figure 1b). A small

DOI: 10.1021/acs.analchem.9b00776
Anal. Chem. 2019, 91, 5433−5445

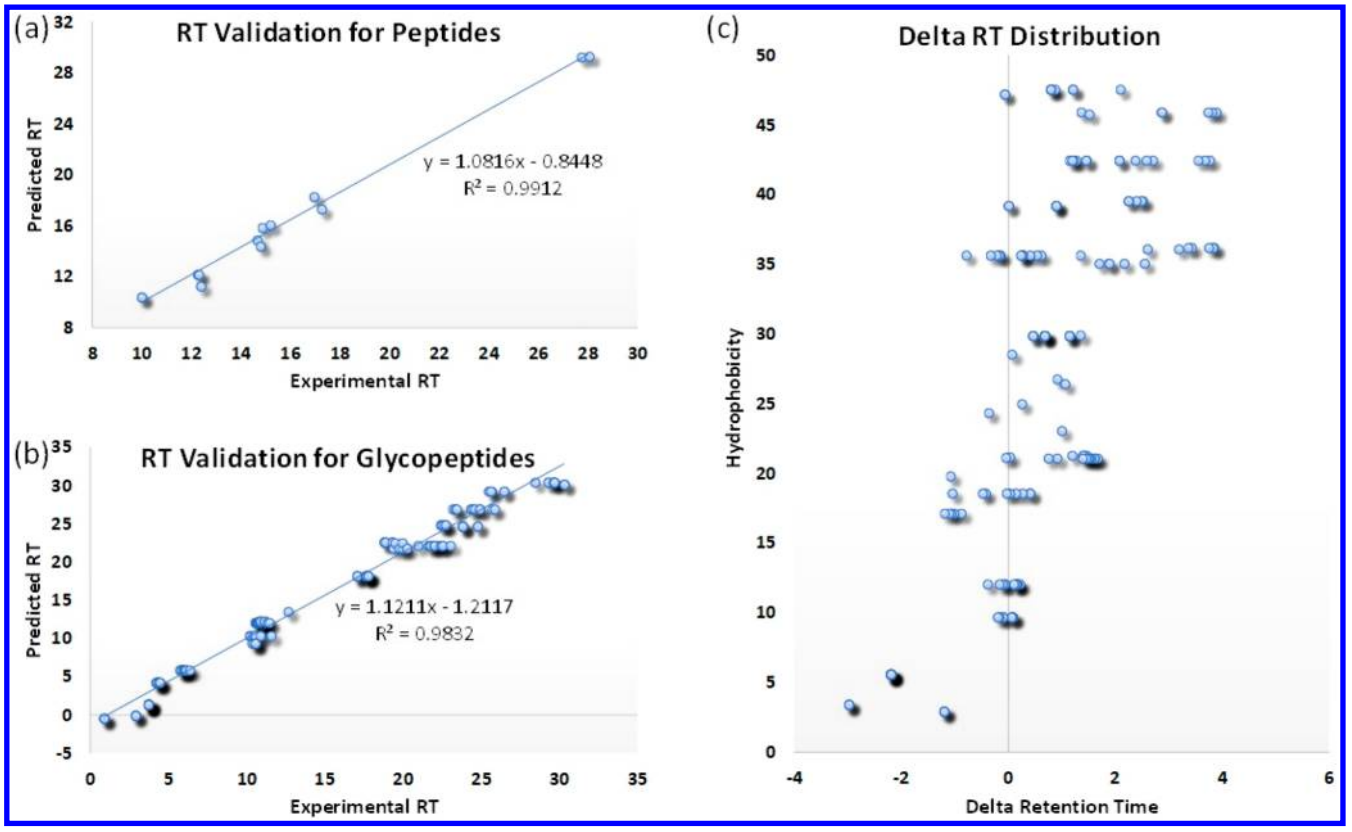

Figure 4. (a) Validation of RT prediction for peptides. (b) Validation of RT prediction for glycopeptides. (c) The delta RTs distribution along with the hydrophobicity values.

percentage of glycopeptides contained high-mannose N-glycans.

For this analysis, trypsin was used as well as a combination of trypsin and Glu-C. Trypsin cleaves proteins at the C-terminus of arginine (R) or lysine (K), while Glu-C cleaves at the C-terminus of glutamic acid (E). Although trypsin is a highly specific enzyme, miss-cleavages can occur due to, for example, PTMs near the cleavage site resulting in large peptides. There are also regions of the polypeptide backbone that lack cleavage sites, producing other large peptides that fall out of the technical mass range or are strongly retained during chromatography. To produce smaller peptides, Glu-C was also used following trypsin to increase the number of detectable glycopeptides. Interestingly, although the total numbers of glycopeptides generated by the methods were nearly the same, there were variations in the specific glycosylation sites and glycopeptides that were generated.

The behavior of complement factor H (CFAH), which is a serum glycoprotein involved in the regulation of the complement system, provides a representative example. Among nine potential N-glycosylation sites, trypsin digestion of the whole serum yielded the glycosylation at five sites, N217, N882, N911, N1029, and N1095 (Figure 2a), of CFAH. No glycopeptides were observed for the other four glycosites, N529, N718, N802, and N822, potentially because their peptide backbones were long. With the dual-enzyme digestion, the site-specific mapping of two additional sites, N529 and N718, were obtained to yield in total seven out of nine glycosylation sites, revealing that the protein is mainly N-glycosylated with complex-type structures.

Another example protein that yielded better results with a combination of both trypsin and Glu-C digestion was complement component 4B (CO4B) (Figure 2b). For this protein, the site N862 was missed in the glycosylation mapping of the tryptic digested serum. Using both trypsin and Glu-C, a shorter peptide containing the site N862 was obtained, and the glycosylation on this site was determined. In total, four out of six glycosylation sites of CO4B were obtained and were shown to be heavily decorated with sialylated-, fucosylated-, and high-mannose-type glycans.

MRM Transitions of Peptides and Glycopeptides. To quantify proteins and glycopeptides in a targeted manner, MRM was developed on an UHPLC-QqQ MS instrument by creating a transition list for glycopeptides and peptides of serum glycoproteins. Proteins were selected that yielded the highest number of glycosylation sites with the highest glycan heterogeneity based on the glycoproteomic analysis. This analysis yielded approximately 50 glycoproteins, which were then selected for MRM analysis. The transitions were constructed from the m/z values of precursor ions as well as the product ions that were further generated from the collision-induced dissociation (CID) spectra. The CID energies were optimized for peptides and glycopeptides based on their m/z values.

Tryptic peptides of the 50 proteins were systematically selected as quantitative peptides and were tested for the lowest coefficient of variation (CV), highest LOD and LOQ, as well as the broadest dynamic ranges. The product ion from CID of each peptide was typically a high-abundance b ion or y ion. In Table 1, the MRM transitions are listed for the quantitative peptides with both quantifiers and qualifiers for nine glycoproteins, including hemopexin (HEMO), kininogen-1 (KNG1), complement factor H (CFAH), CO4B, vitronectin (VTNC), complement component 5 (CO5), angiotensinogen

DOI: 10.1021/acs.analchem.9b00776
Anal. Chem. 2019, 91, 5433−5445

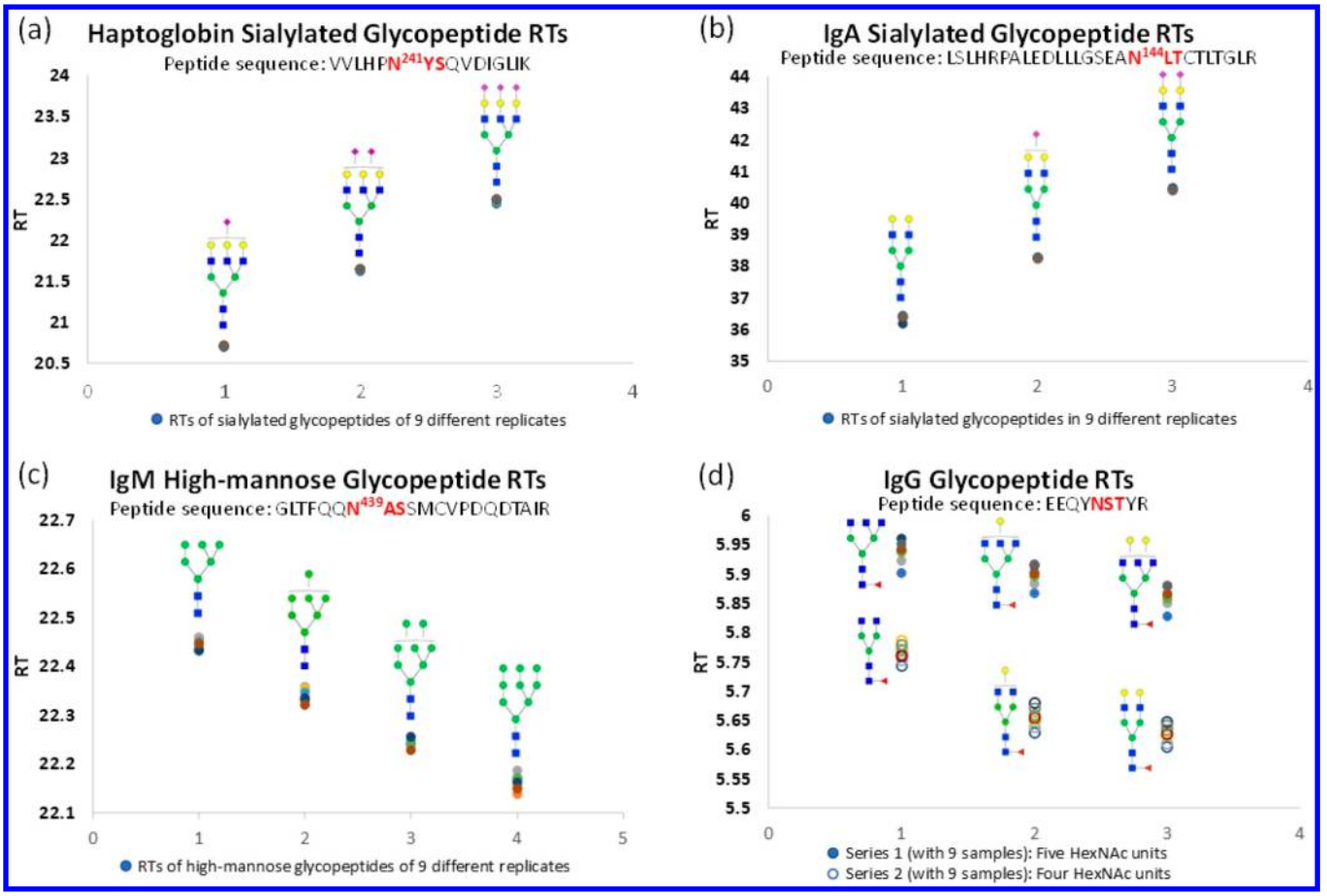

Figure 5. (a) The RT variation trend of sialylated haptoglobin glycopeptides along with the number of sialic acids in the N-glycans. (b) The RT variation trend of sialylated IgA glycopeptides along with the number of sialic acids in the N-glycans. (c) The RT variation trend of high-mannosylated IgM along with the number of mannoses in the N-glycans. (d) The RT variation trend of IgG glycopeptides along with the number of HexNAcs and hexoses. Different colors represent different replicates.

Table 3. Summary of the R^2 Values, Linear Ranges, LOQs, and LODs of the Quantitation Methods

protein	peptide	regression line	R^2	linear range (nM)	LOQ (fmol)	LOD (fmol)
HEMO	NFPSPVDAAFR	$y = 4.10 \times 10^{06}x + 7.70 \times 10^{02}$	0.998	9.52−4760	38.1	3.81
KNG1	YFIDFVAR	$y = 1.74 \times 10^{06}x + 6.09 \times 10^{02}$	0.998	9.17−4580	36.7	18.3
CFAH	IDVHLVPDR	$y = 6.63 \times 10^{05}x - 1.29 \times 10^{03}$	0.999	6.04−3020	24.2	12.1
CO4B	VLSLAQEQVGGSPEK	$y = 3.99 \times 10^{05}x + 1.82 \times 10^{03}$	0.995	6.38−6380	25.5	2.55
VTNC	FEDGVLDPDYPR	$y = 3.47 \times 10^{06}x + 1.33 \times 10^{01}$	0.998	2.67−1330	10.7	5.33
CO5	GIYGTISR	$y = 9.92 \times 10^{05}x + 1.06 \times 10^{03}$	0.999	3.16−3160	12.6	1.26
ANGT	SLDFTELDVAAEK	$y = 1.55 \times 10^{06}x + 2.49 \times 10^{02}$	0.997	3.23−1610	12.9	6.45
ANT3	IEDGFSLK	$y = 2.09 \times 10^{06}x - 6.74 \times 10^{02}$	0.996	2.07−2070	8.30	1.66
CFAI	IVIEYVDR	$y = 1.75 \times 10^{06}x + 4.24 \times 10^{03}$	0.991	6.82−3410	27.3	2.73

(ANGT), antithrombin III (ANT3), and complement factor I (CFAI) as examples.

The MRM transitions of glycopeptides were developed from the glycomap produced from the glycoproteomic analysis. The m/z values of the target glycopeptides were used as the precursor ions. To cover glycoforms that were not observed in the maps but were biologically possible and may be found in some disease states, the m/z values of the glycopeptides for proteins that have been previously reported in literature[21−27] together with the glycopeptides containing theoretical glycoforms were also included with their theoretical precursor ions. For theoretical glycopeptides, we took an existing glycan on a site and extended it by the addition of various monosaccharides depending on the glycan types. For high mannose, we added or subtracted mannoses, consistent with the biosynthesis. For complex, we added and subtracted fucoses or sialic acids depending on the putative biosynthesis process. Common high-abundance fragment ions of glycopeptides, including m/z values of 204.08 (HexNAc), 366.14 ($Hex_1HexNAc_1$), and 292.09 (Neu5Ac), were used as the product ions. In the quantitation, the transitions from precursor to m/z 366.14 were used as quantifiers, while those from precursor to m/z 204.08 were used as qualifiers.

Standard MRM probes were used for all transitions throughout the chromatographic separation, thereby limiting the total number of transitions. To increase the number of targeted compounds, dMRM was used, which entails monitoring distinct transitions at specific elution periods. In

DOI: 10.1021/acs.analchem.9b00776
Anal. Chem. 2019, 91, 5433−5445

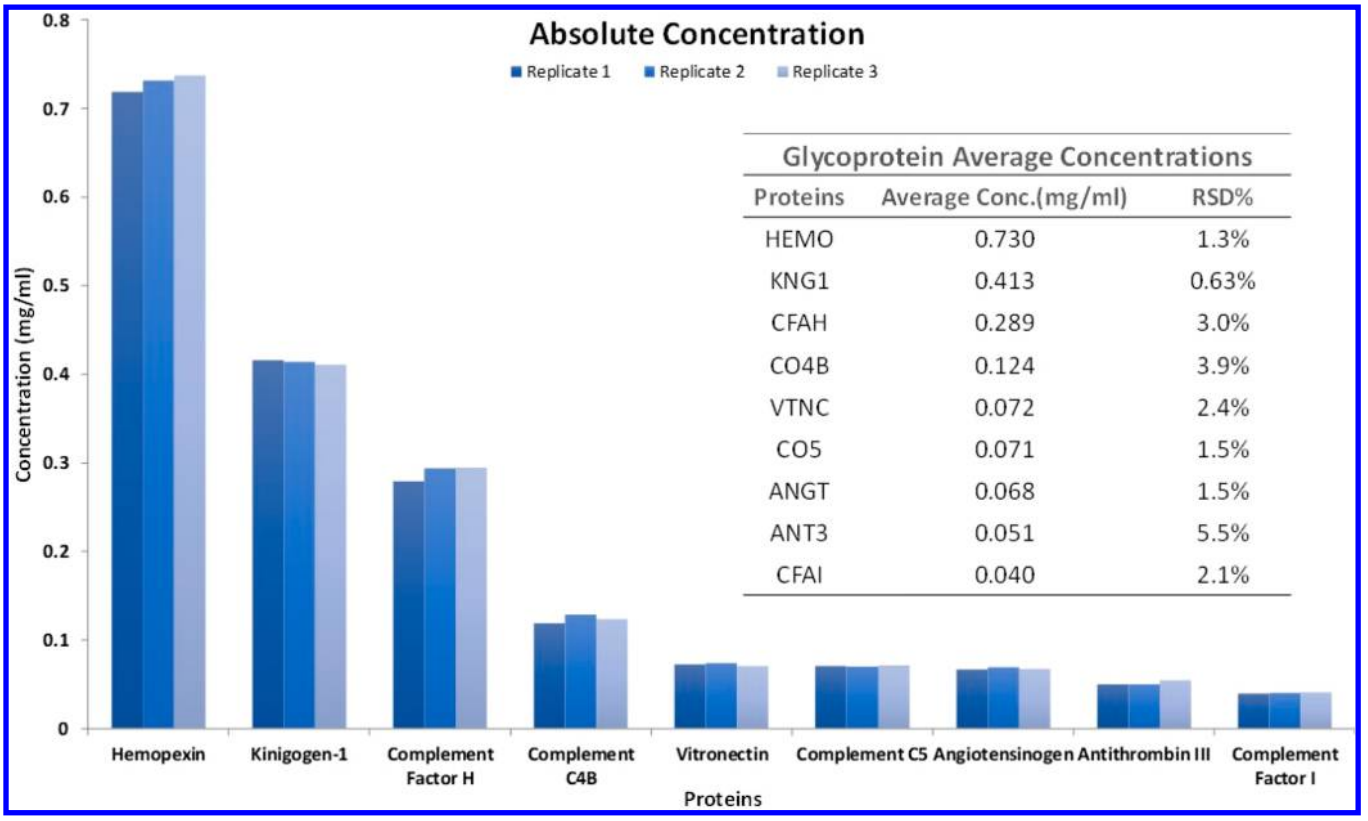

Glycoprotein Average Concentrations

Proteins	Average Conc.(mg/ml)	RSD%
HEMO	0.730	1.3%
KNG1	0.413	0.63%
CFAH	0.289	3.0%
CO4B	0.124	3.9%
VTNC	0.072	2.4%
CO5	0.071	1.5%
ANGT	0.068	1.5%
ANT3	0.051	5.5%
CFAI	0.040	2.1%

Figure 6. Concentration estimation of nine proteins determined in triplicates together with the average concentrations of nine proteins and RSD% values of quantitation.

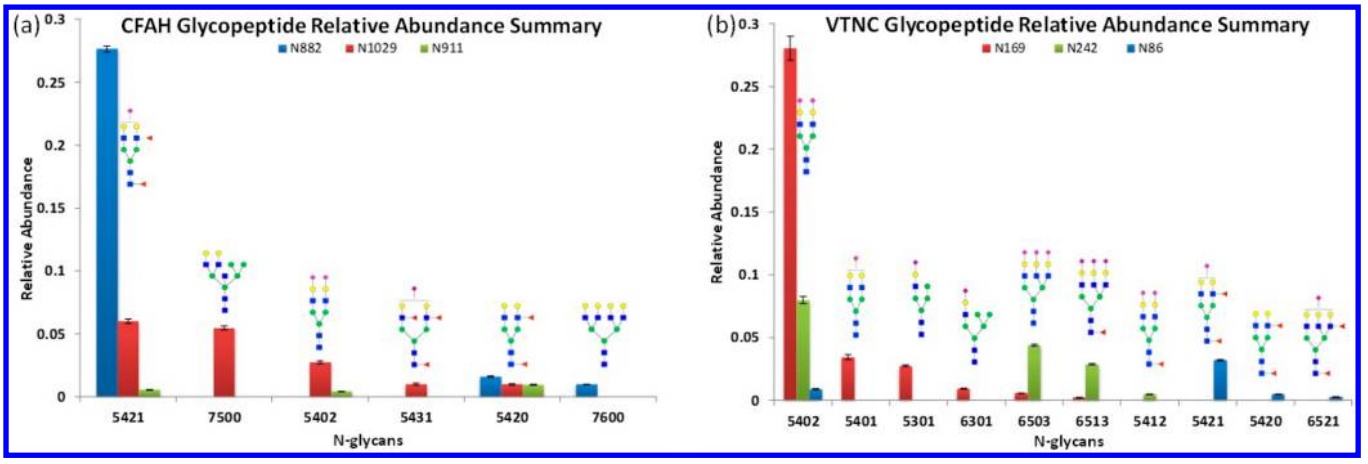

Figure 7. Determination of glycosylation degree of (a) CFAH and (b) VTNC.

dMRM, the transitions are probed at the RT of each precursor ion with a delta RT of ±0.75 to 1 min. The method allows for a significant increase in the number of transitions compared to standard MRM for the same chromatographic period. In this analysis, we used dMRM to monitor around 600 distinct glycopeptides, and we predict that it can be used for over 1000.

Predictive Glycopeptidomics and dMRM for Enhanced Glycopeptide Coverage. Dynamic MRM increases the number of transitions in a method by monitoring peptides and glycopeptides at their expected elution times. Given that glycans that may be present may have minor variations to those observed, such as a loss or presence of fucose, hexose, or sialic acid, a predictive method to account for these species was developed. We found that the glycopeptide RTs vary only slightly from the parent peptide on a C18 column. We, therefore, predicted the RT of the peptide by studying the RT characteristics of observed species and developed transitions for the corresponding virtual glycopeptides. To determine RTs of the parent peptides, the following strategy was employed. First, a series of standard peptides (12 are listed in Table 2) were obtained and used to determine the variation of RTs in a 50 min LC gradient. The hydrophobicity values of the standards were obtained using the method previously described by Spicer et al. on the Web site SSRCalc.[28] The RTs of the peptide standards were determined using the UHPLC conditions. With the experimental RTs and hydrophobicity values of peptides, a curve of RT vs hydrophobicity was generated (Figure 3), revealing that the RTs of the

DOI: 10.1021/acs.analchem.9b00776
Anal. Chem. 2019, 91, 5433−5445

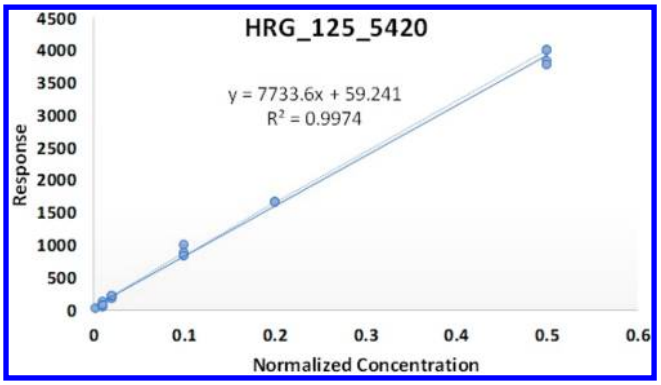

Figure 8. Estimation of linearity of glycopeptide quantitation.

peptides vary remarkably linearly when plotted against the hydrophobicity values. Linear regression yielded a retention time calibration curve with an excellent R^2 value (Figure 3). In general, we found that the RT of the glycopeptide on C18 columns matched well with the RT of the peptide because glycans are not retained in C18 stationary phases. Thus, this retention time calibration curve was used to predict the RTs of the glycopeptides, which varied only slightly (less than 2 min) from the peptide backbones.

To validate the prediction method, the experimental RTs were compared to the predicted RTs using a ten-protein standard. The experimental RTs of glycopeptides were determined using UHPLC-QqQ in the MRM scan mode. The theoretical RTs were calculated using the computed linear regression line and hydrophobicity values of the glycopeptides. The predicted RTs were plotted against the experimental RTs for both peptides and glycopeptides (Figure 4a,b, respectively). The linear regression of the corresponding plots yielded high R^2 values with slopes of 1.08 and 1.12, respectively.

The glycosylation affected the RTs in a systematic manner also. To gain a better understanding of this behavior, the hydrophobicity values were plotted against the differences between the experimental RTs and the predicted RTs (delta RT, Figure 4c). When the peptide backbone was more hydrophobic, the glycans increased the RTs of the glycopeptide relative to the parent peptide. While when the peptides are more hydrophilic, the glycans decreased the RTs. Due to the slight variation of glycopeptide RTs from their predicted RTs, the time windows of transitions with RTs during 0−10 and 30−40 min were set with larger values ranging from 2 to 3 min.

The RTs of certain glycan types also appeared to follow the trend as illustrated in Figure 5. N-glycan composition is denoted as the number of different monosaccharides [ABCD] according to $Hexose_AHexNAc_BFucose_CNeu5Ac_D$. The data suggest that sialylation on the glycoform delayed the RT of the glycopeptide on the C18 column, and some of the most representative glycopeptides are demonstrated here to illustrate the trend. For example, the asparagine (N241) of haptoglobin in the consensus sequence of NYS was glycosylated with sialylated N-glycans 6501, 6502, and 6503. With the increasing number of the sialic acid, the RTs of glycopeptides increased by around one minute (Figure 5a). Similarly, the N-glycans on IgA, including 5400, 5401, and 5402 on N144, differed in RTs accordingly (Figure 5b). High-mannose-type glycans also had variable RTs depending on the number of mannoses. As shown in Figure 5c, the high-mannose-type glycans on N439 of IgM varied the RTs of the respective glycopeptide by increasing systematically with the increasing number of mannoses. Figure 5d illustrates the variations in glycopeptide RTs with both the number of HexNAc and Hexose. Two series of glycopeptides on the IgG glycosylation site were shown where the series 1 (illustrated with dots) were glycopeptides decorated by glycans with 5 HexNAc units, and the series 2 (illustrated with circles) were glycopeptides decorated by glycans with 4 HexNAc units. With the increasing number of HexNAc, the RTs of glycopeptides increased by 0.25 min. When comparing within each series, the RTs of glycopeptides decreased systematically with the increasing number of hexoses.

Quantitation of Proteins Using dMRM. The absolute quantitation of selected glycoproteins was conducted using available standards with the developed dMRM method (Table 1). Although protein standards would be desirable for all proteins, they are limited by either availability or appropriate purity, thereby limiting the number of proteins that can be quantified in absolute terms. For each glycoprotein, two peptides are used for quantitation, one as a qualifier and the other as a quantifier. Both of the precursor ions and the product ions of each peptide for nine standards are listed in Table 1. The standards were serially diluted and used to build calibration curves that were employed to quantify these glycoproteins in serum. Table 3 shows the linear ranges, LOQs, and LODs of the quantitation of these proteins with the method. The calibration curve of each quantitative peptide showed high linearity (R^2 > 0.99). To quantify proteins that have large concentration variations, the linear range should cover a wide range. This method gave linear scales spanning 3−4 orders of magnitude. Additionally, all the LOQs and LODs were at the femtomole level, demonstrating the high sensitivity of the technique.

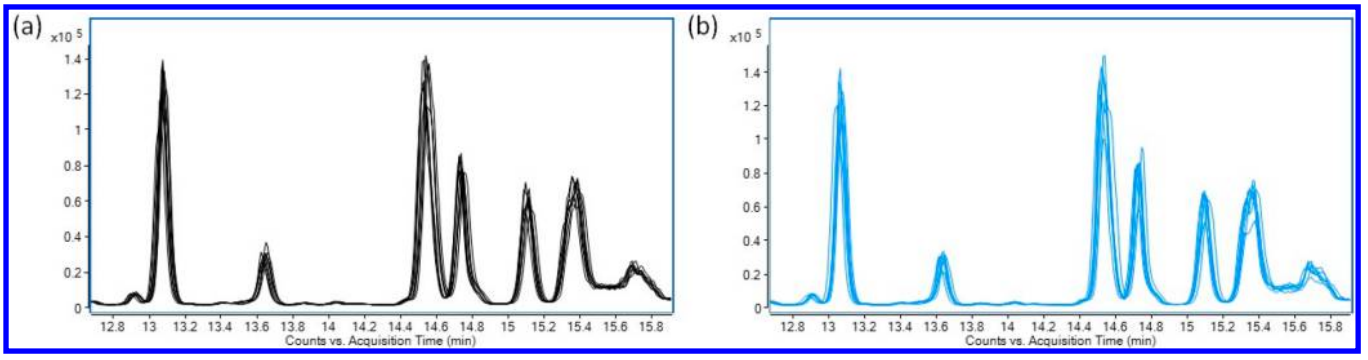

Figure 9. Validation of the method reproducibility including the (a) instrument reproducibility and (b) the tryptic digestion reproducibility.

DOI: 10.1021/acs.analchem.9b00776
Anal. Chem. 2019, 91, 5433−5445

Table 4. Library of the 50 Glycoproteins Together with the Numbers of Glycosylation Sites and Glycopeptides Monitored with Quantitation in the 50 min dMRM Method

glycorotein	no. of sites	no. of glycopeptides	glycoprotein	no. of sites	no. of glycopeptides
1_A1AT_Alpha-1-antrypsin	3	11	26_CO6_ComplementComponetC6	2	10
2_A1BG_Alpha-1B-glycoprotein	1	6	27_CO8A_ComplementComponetC8AChaing	1	5
3_A2GL_Leucine-richAlpha-2-glycoprotein	1	5	28_CO8B_ComplementComponetC8BChain	2	12
4_A2HSG_Alpha-2-HS-glycoprotein	3	23	29_FINC_Fibronectin	3	11
5_A2MG_Alpha-2-macroglobulin	5	25	30_HEMO_Hemopexin	2	15
6_AACT_Alpha-1-antichymotrypsin	1	5	31_HEP2_HeparinCofactor2	2	9
7_AFAM_Afamin	1	8	32_HP_Haptoglobin	3	31
8_AGP_Alpha-1-acid glycoprotein	5	47	33_HRG_Histidine-richGlycoprotein	3	6
9_ANGT_Angiotensinogen	2	5	34_IgA_Immunoglobulin A	2	17
10_ANT3_Antithromnin-III	2	10	35_IGG_Immunoglobulin G	1	26
11_APOCIII_Apolipoprotein CIII	1	14	36_IgM_Immunoglobulin M	3	21
12_APOD_ApolipopioteinD	1	16	37_ITIH1_Inter-alpha-trypsinInhibitorHeavyChainH1	1	5
13_APOH_Beta-2-glycoprotein1	1	6	38_ITIH4_Inter-alpha-trypsinInhibitorHeavyChainH4	1	5
14_APOM_ApolipoproteinM	1	8	39_KLKB1_PlasmaKallikrein	2	10
15_ATL_3ADAMTS-likeProtein3	1	14	40_KNG1_Kininogen-1	3	9
16_ATRN_Attractin	5	9	41_KPCD3_Serine/threonine-proteinKinaseD3	1	6
17_CAN3_Calpain-3	1	5	42_LUM_Lumican	1	8
18_CERU_Ceruloplasmin	4	24	43_PON1_SerumParaoxonase/arylesterase1	2	10
19_CFAH_ComplementFactorH	3	23	44_SEPP1_SelenoproteinP	2	5
20_CFAI_ComplementFactorI	3	25	45_TF_Transferrin	2	11
21_CLUS_Clusterin	3	12	46_THBG_Thyroxine-bindingGlobulin	1	6
22_CO2_ComplementC2	1	5	47_THRB_Prothrombin	2	5
23_CO4A_ComplementC4-A	2	5	48_UN13A_Protein unc-13HomologA	1	12
24_CO4B_ComplementC4-B	2	6	49_VINC_Vitronectin	3	20
25_CO5_ComplementC5	1	7	50_ZA2G_Zinc-alpha-2-glycoprotein	3	11
			total	103	610

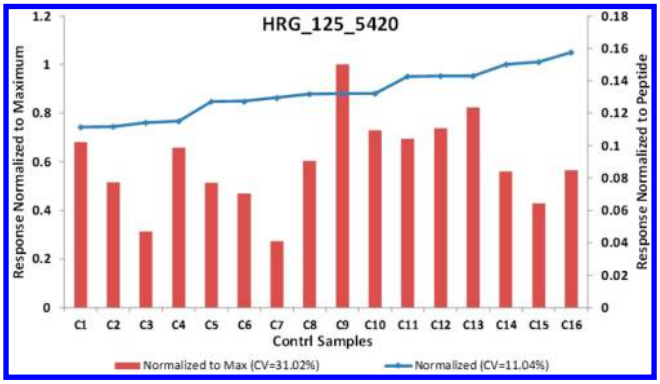

Figure 10. Application of the dMRM to 16 healthy human serum samples for the quantitation of peptide HRG_125_5420.

The method was validated with triplicate measurements of the standard proteins in serum, with the measured concentrations of each protein in each trial summarized in Figure 6. The table in Figure 6 lists the average concentrations and the relative standard deviations (RSD%) of the measurement of standard proteins. Among the standards, the protein with the highest concentration (0.73 mg/mL) in serum was hemopexin, which matched well the concentration (0.77 mg/mL) reported in the literature.[29] The concentration of the lowest-abundant protein CFAI was determined to be 0.040 mg/mL in serum with our method, which was reported as 0.035 mg/mL in a previous study.[30] Overall, the RSD% values ranged from 0.63 to 5.5%, showing the high reproducibility of the method.

Quantitation of Glycopeptides with dMRM. There are almost no available standards for individual glycopeptides, making absolute quantitation of glycopeptides unfeasible; therefore, we measure fold-changes for relative quantitation instead. To separate the changes of protein abundances from variations in glycan expression, the abundance (as measured by ion counts) of a glycopeptide was normalized to the abundance (ion counts) of the quantitating peptide of that protein. Without this normalization, the changes in glycopeptide abundances could be due to the variations in protein concentration rather than the expression of glycosylation on specific sites.

Results for two glycoproteins, CFAH and VTNC, are shown in Figure 7 as illustrative examples. Because peptides are generally better ionized than glycopeptides, and the glycopeptide signals are spread over several glycoforms, the ratio of glycopeptide to peptide ion abundances are typically much lower than one. For the protein CFAH, three glycopeptides with N-glycans 5421, 5420, and 7600 on site N882, three glycopeptides with N-glycans 5420, 5421, and 5402 on site N911, and six glycopeptides with N-glycans 5421, 7500, 5402, 5431, and 5420 on site N1029 were quantified (Figure 7a). The glycosylation of the other four sites was not quantified here, possibly due to the low relative abundances of glycopeptides or the low occupancy of the sites. Similarly, the glycopeptide abundances on three sites, including N86, N169, and N242 of the protein VTNC, were acquired with the glycans being highly sialylated with the highest abundance corresponding to 5402 (Figure 7b).

The LOQ could not be determined due to a lack of standards; however, the linear range can be estimated using

DOI: 10.1021/acs.analchem.9b00776
Anal. Chem. 2019, 91, 5433−5445

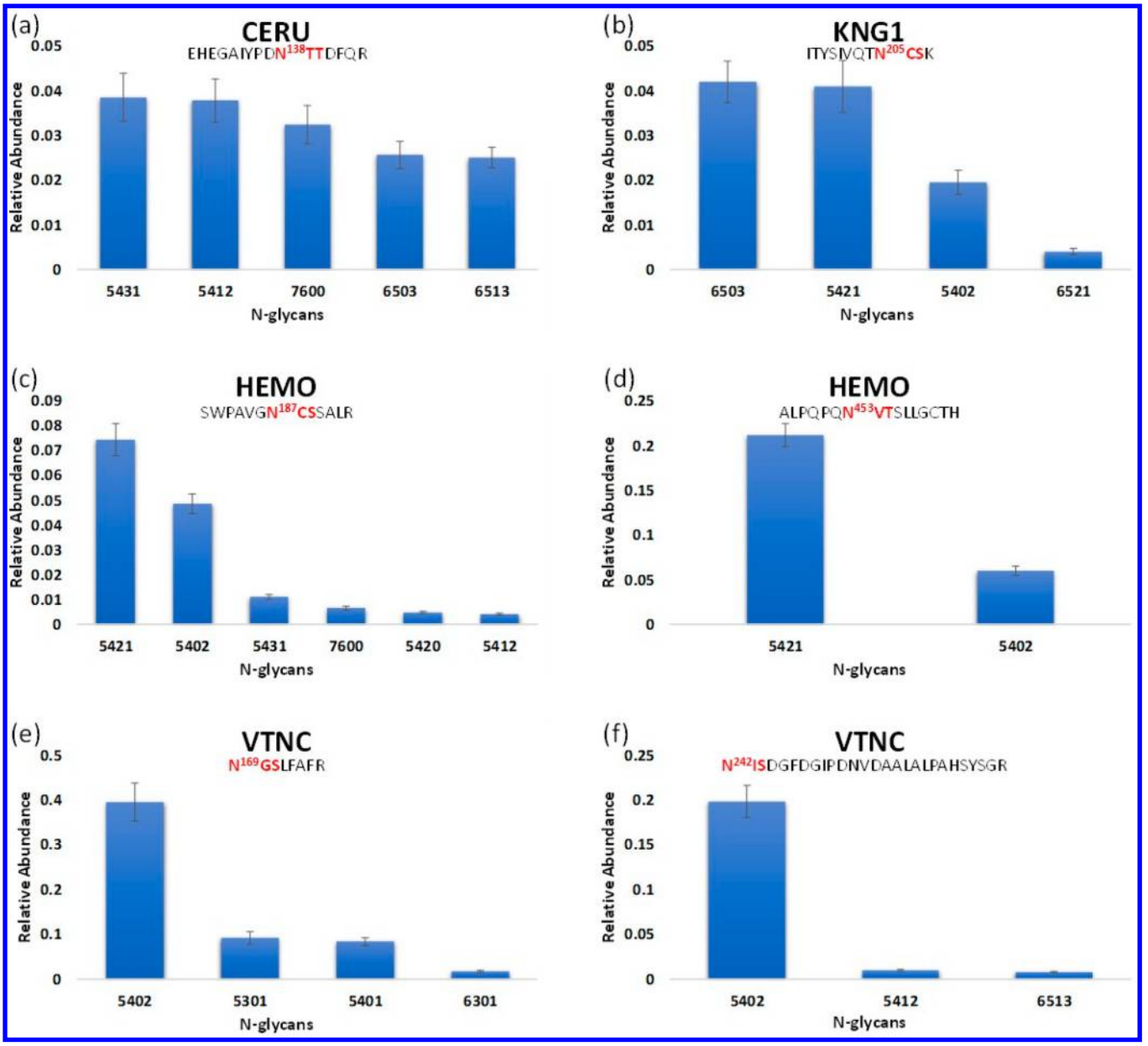

Figure 11. Normalized N-glycopeptide abundance of four proteins. (a) Ceruloplasmin, site 138; (b) kininogen, site 205; (c, d) hemopexin, sites 187 and 453; and (e, f) vitronectin, sites 169 and 242. The error bar represents the biological variation.

serial dilution of serum. When a standard serum sample was diluted from 1× to 500×, the linearity of the glycopeptide abundance relative to the protein abundance could be obtained. A glycopeptide of histidine-rich glycoprotein denoted as HRG_125_5420, (protein name_site_glycan composition) is used to illustrate the linearity of the quantitation. The responses of the glycopeptide in serum samples with varying dilution were plotted with normalized concentrations (Figure 8), yielding an R^2 value of 0.997, indicating high linearity over the dilution range.

To validate the repeatability of this method, both the instrumentation and sample digestion repeatabilities were evaluated. To determine the intraday instrumentation reproducibility, one tryptic-digested serum sample was prepared and injected into the instrument nine times within one day. The instrument showed excellent repeatability with a CV less than 5% (Figure 9a). The sample digestion reproducibility was then evaluated by conducting nine trypsin digestions on one serum sample. The digestion with trypsin also showed high reproducibility with a CV less than 10% (Figure 9b).

Biological Variation in Site-Specific Glycan Expression. By employing all of the strategies described above, a dMRM method monitoring nearly 800 glycopeptides and peptides of 50 glycoproteins in serum was established using a 50 min LC gradient. Previously, Hong et al.[17] developed the dMRM method for the quantitation of seven glycoproteins in a 15 min LC gradient. In order to increase the peak capacity of the method, the LC gradient was extended to 50 min, which allowed us to analyze 50 proteins at once. The number of glycosylation sites and unique glycopeptides of each glycoprotein is summarized in Table 4.

Many of the proteins contained in the method have established biological functions that could be affected by

DOI: 10.1021/acs.analchem.9b00776
Anal. Chem. 2019, 91, 5433−5445

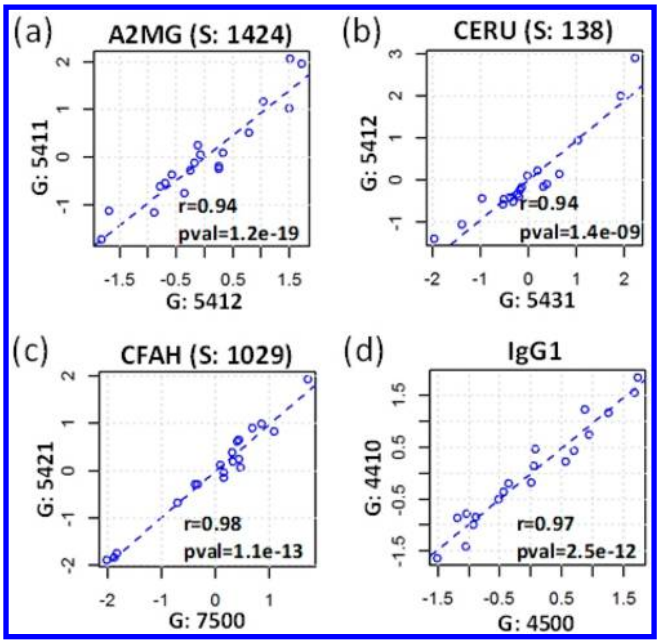

Figure 12. Intraprotein correlation between the glycans on (a) alpha-2-macroglobulin, site 1424; (b) ceruloplasmin, site 138; (c) CFAH, site 1029; and (d) IgG1.

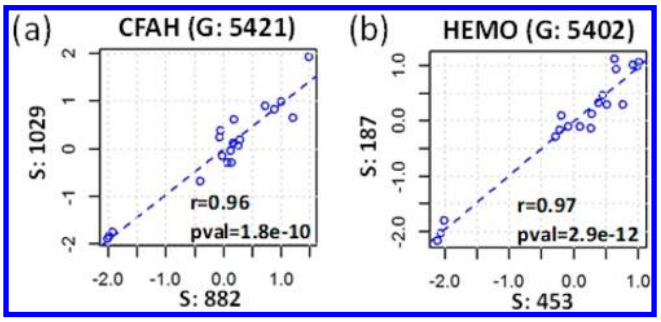

Figure 13. Intraprotein correlation of the same glycan on different sites. (a) Correlation of the glycan 5421 on the sites 1029 and 882 of the protein CFAH. (b) Correlation of the glycan 5402 on the sites 187 and 453 of the protein HEMO.

diseases. For example, there are six complement proteins, including C2, C4A, C4B, C5, C6, and C8, in this list which are involved in the innate immune system.[31] Serum complement C3 and C4 levels were significantly increased in patients with severe chronic spontaneous urticaria (CU) compared to healthy subjects and patients with milder forms of the disease.[32] Although the different expression levels of these proteins make them potential biomarkers of the disease, the methods they were identified with are more specific to one certain disease and might not be able to be applied to the biomarker discovery in a large sample set. The large number of glycopeptides that this method can simultaneously monitor theoretically increases the potential of the technique to identify a biomarker with predictive utility.

To determine the validity and robustness of the method, it was applied to 16 healthy human serum samples. To eliminate the variations in abundances of glycopeptides due to changes in protein concentrations, the abundances of glycopeptides were normalized to the abundances of the quantitating nonglycosylated peptides of the respective proteins, denoted as "response normalized to peptide" (RNP). The results

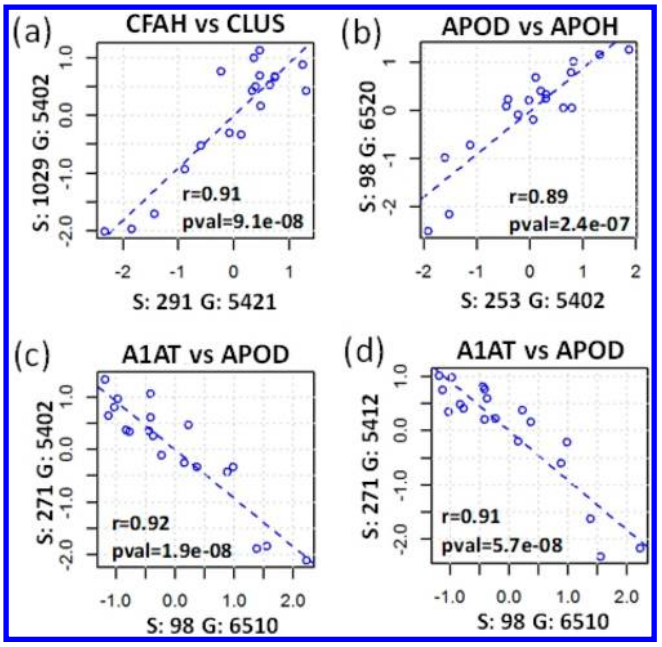

Figure 14. Interprotein correlations between (a) CFAH and clusterin, (b) APOD and APOH, (c) and (d) A1AT and APOD.

generated from this normalization method were compared with another normalization method, denoted as "response normalized to maximum" (RNM), or the relative abundances of glycopeptides normalized to the most abundant glycopeptide for that peptide or site. For example, Figure 10 is the quantitation results for the glycopeptide HRG_125_5420. This figure reveals that for this glycopeptide, the RNP and RNM methods yielded CVs of 11 and 31%, respectively, across different samples.

The abundances of glycopeptides of 50 glycoproteins were determined using RNP, and the site-specific glycosylation of four example glycoproteins, including CERU, KNG1, HEMO, and VTNC, is shown in Figure 11. The relative abundances of the most common N-glycan structures are included here as well as the glycopeptides and glycosylation sites. The relative abundances of CERU N-glycans shown in Figure 11a were close, varying in the range of 0.025−0.04 with the biantennary N-glycan 5431 being the most abundant. For the protein KNG1 (Figure 11b), the relative abundances of N-glycans varied more, with the triantennary N-glycan 6503 as the most abundant. Two glycosylation sites at asparagine 187 and 453 of the protein HEMO were determined for the relative abundances of different glycoforms (Figure 11c,d). The most abundant glycan at site 187 was the biantennary N-glycan 5421, and the next most abundant was fucosylated glycan 5402. The glycosylation site 453 had two glycoforms quantitated for their relative abundances, with the glycan 5421 being more abundant than glycan 5402. In addition, two glycosylation sites, 169 and 242, on VTNC were quantified. For both sites, the glycan 5402 had the highest relative abundance (Figure 11e,f).

With the availability of quantitative glycopeptidomic data, we next examined whether specific correlations existed between the relative abundance of different site-specific glycosylations of serum proteins. Thus, glycan−glycan correlations were calculated, and *p*-values were adjusted for multiple testing using the FDR method. Notably, several types of strong correlations were identified. First, intrasite glycan

DOI: 10.1021/acs.analchem.9b00776
Anal. Chem. 2019, 91, 5433−5445

correlations were common. Examples obtained from the analysis of four different proteins (A2MG, CERU, CFAH, and IgG1) are shown in Figure 12. For the protein A2MG, the fucosylated and sialylated glycans 5411 and 5412 at site 1424 strongly correlated with one another. Similar correlations were observed for glycans 5412 and 5431 at the site 138 of CERU. There were also correlations noted between neutral glycans, 7500 of CFAH and 4500 of IgG1, and decorated glycans, such as 5421 of CFAH and 4410 of IgG1, respectively.

Intraprotein correlations between the same glycan structure on different sites of a glycoprotein were also detected and are presented in Figure 13, with proteins CFAH and HEMO as examples. For CFAH, the relative abundance of the glycan 5421 at position 882 correlated with its abundance at position 1029. In addition, for HEMO, the glycan 5402 at sites 453 and 187 correlated well with each other.

There were also both positive and negative interprotein glycan correlations. Glycan 6520 at position 98 of apolipoprotein D (APOD) correlated with the glycan 5402 at site 253 of apolipoprotein H (APOH). APOD also had glycan 6510 at site 98 that negatively correlated with glycans 5402 and 5412 at site 271 of A1AT (Figure 14). These correlations are intriguing and could be due to several possibilities. One possibility is that these correlations between glycopeptides suggest a connection in functions between different sites and different proteins. It has long been known that both proteins APOD and APOH play essential roles in regulating lipoproteins and act as cofactors of lipoprotein lipase.[33] Similarly, He et al.[34] found that APOAI and A1AT were degraded during inflammation, suggesting that they are both acute-phase proteins.

CONCLUSION

The combination of glycomic mapping of proteins in serum coupled with dMRM provides a platform for biomarker research and discovery; in addition, its utility is broader and can be used to understand fundamental processes in glycobiology. We demonstrate the ability to comprehensively map site-specific glycosylations across 200 glyco-sites of 50 serum glycoproteins. The large number of glycopeptides can be quantitatively monitored using dynamic MRM. Although the method is targeted, the glycopeptide coverage is large and compares well with that of untargeted glycoproteomic analysis at least for serum, where the glycopeptide enrichment yields approximately the same number of glycopeptides. More importantly, the dMRM method is quantitative with high sensitivity and selectivity over a wide dynamic range. Furthermore, the described sample preparation is rapid and comprehensive, generating a large repertoire of serum glycopeptides with no sample cleanup.

Quantitative glycoproteomic will have wide utility in biomarker discovery but also in understanding fundamental biological processes in serum, which is made possible by tracking a large cohort of glycopeptides in a quantitative manner. This method could also be applied to glycoproteins in any tissues, with the targeted glycopeptides matched for specific tissues. This method has broad utility yielding both protein and glycopeptide abundances. Furthermore, the quantitative nature of the analysis allowed us to mine our data sets for the presence of site-specific glycan−glycan correlations. While, the roots of these correlations are not yet known, their strong dependency suggests a biochemical behavior of glycans that has not been and could not be previously explored.

ASSOCIATED CONTENT

Supporting Information

The Supporting Information is available free of charge on the ACS Publications website at DOI: 10.1021/acs.analchem.9b00776.

Full transition list (XLSX)

AUTHOR INFORMATION

Corresponding Author

*E-mail: cblebrilla@ucdavis.edu.

ORCID

Qiongyu Li: 0000-0003-3654-0378
Muchena J. Kailemia: 0000-0001-9359-1038
Gege Xu: 0000-0002-0792-2636
Carlito B. Lebrilla: 0000-0001-7190-5323

Notes

The authors declare no competing financial interest.

ACKNOWLEDGMENTS

Funding provided by the National Institutes of Health (grant R01GM049077) for Dr. Lebrilla's laboratory is gratefully acknowledged. Dr. Haj's laboratory is funded by R01DK095359 and P42ES004699. Dr. Haj is the Co-Leader of the Endocrinology and Metabolism Core of UCD, Mouse Metabolic Phenotyping Center, which is funded by U24DK092993.

REFERENCES

(1) Füzéry, A. K.; Levin, J.; Chan, M. M.; Chan, D. W. *Clin. Proteomics* **2013**, *10* (1), 13.
(2) Strimbu, K.; Tavel, J. A. *Curr. Opin. HIV AIDS* **2010**, *5* (6), 463−466.
(3) Kailemia, M. J.; Park, D.; Lebrilla, C. B. *Anal. Bioanal. Chem.* **2017**, *409* (2), 395−410.
(4) Meezan, E.; Wu, H. C.; Black, P. H.; Robbins, P. W. *Biochemistry* **1969**, *8* (6), 2518−2524.
(5) Maverakis, E.; Kim, K.; Shimoda, M.; Gershwin, M. E.; Patel, F.; Wilken, R.; Raychaudhuri, S.; Ruhaak, L. R.; Lebrilla, C. B. *J. Autoimmun.* **2015**, *57*, 1−13.
(6) Yin, B. W.; Lloyd, K. O. *J. Biol. Chem.* **2001**, *276* (29), 27371−27375.
(7) Catalona, W. J.; Richie, J. P.; Ahmann, F. R.; Hudson, M. A.; Scardino, P. T.; Flanigan, R. C.; Dekernion, J. B.; Ratliff, T. L.; Kavoussi, L. R.; Dalkin, B. L. *J. Urol.* **1994**, *151* (5), 1283−1290.
(8) An, H. J.; Froehlich, J. W.; Lebrilla, C. B. *Curr. Opin. Chem. Biol.* **2009**, *13* (4), 421−426.
(9) Ruhaak, L. R.; Xu, G.; Li, Q.; Goonatilleke, E.; Lebrilla, C. B. *Chem. Rev.* **2018**, *118* (17), 7886−7930.
(10) de Leoz, M. L. A.; An, H. J.; Kronewitter, S.; Kim, J.; Beecroft, S.; Vinall, R.; Miyamoto, S.; de Vere White, R.; Lam, K. S.; Lebrilla, C. *Dis. Markers* **2008**, *25* (4−5), 243−258.
(11) Alley, W. R.; Vasseur, J. A.; Goetz, J. A.; Svoboda, M.; Mann, B. F.; Matei, D. E.; Menning, N.; Hussein, A.; Mechref, Y.; Novotny, M. V. *J. Proteome Res.* **2012**, *11* (4), 2282−2300.
(12) Drabik, A.; Bodzon-Kulakowska, A.; Suder, P.; Silberring, J.; Kulig, J.; Sierzega, M. *J. Proteome Res.* **2017**, *16* (4), 1436−1444.
(13) Zeng, X.; Hood, B. L.; Sun, M.; Conrads, T. P.; Day, R. S.; Weissfeld, J. L.; Siegfried, J. M.; Bigbee, W. L. *J. Proteome Res.* **2010**, *9* (12), 6440−6449.
(14) Liu, T.; Liu, D.; Liu, R.; Jiang, H.; Yan, G.; Li, W.; Sun, L.; Zhang, S.; Liu, Y.; Guo, K. *Sci. Rep.* **2017**, *7*, 38918.

DOI: 10.1021/acs.analchem.9b00776
Anal. Chem. 2019, 91, 5433−5445

(15) Ahn, Y. H.; Lee, J. Y.; Lee, J. Y.; Kim, Y.-S.; Ko, J. H.; Yoo, J. S. *J. Proteome Res.* **2009**, *8* (9), 4216−4224.
(16) Hong, Q.; Lebrilla, C. B.; Miyamoto, S.; Ruhaak, L. R. *Anal. Chem.* **2013**, *85* (18), 8585−8593.
(17) Hong, Q.; Ruhaak, L. R.; Stroble, C.; Parker, E.; Huang, J.; Maverakis, E.; Lebrilla, C. B. *J. Proteome Res.* **2015**, *14* (12), 5179−5192.
(18) Liebler, D. C.; Zimmerman, L. J. *Biochemistry* **2013**, *52* (22), 3797−3806.
(19) Lange, V.; Picotti, P.; Domon, B.; Aebersold, R. *Mol. Syst. Biol.* **2008**, *4* (1), 222.
(20) Ruhaak, L. R.; Kim, K.; Stroble, C.; Taylor, S. L.; Hong, Q.; Miyamoto, S.; Lebrilla, C. B.; Leiserowitz, G. *J. Proteome Res.* **2016**, *15* (3), 1002−1010.
(21) Takakura, D.; Harazono, A.; Hashii, N.; Kawasaki, N. *J. Proteomics* **2014**, *101*, 17−30.
(22) Nilsson, J.; Rüetschi, U.; Halim, A.; Hesse, C.; Carlsohn, E.; Brinkmalm, G.; Larson, G. *Nat. Methods* **2009**, *6*, 809.
(23) Ji, E. S.; Hwang, H.; Park, G. W.; Lee, J. Y.; Lee, H. K.; Choi, N. Y.; Jeong, H. K.; Kim, K. H.; Kim, J. Y.; Lee, S.; Ahn, Y. H.; Yoo, J. S. *Anal. Bioanal. Chem.* **2016**, *408* (27), 7761−7774.
(24) Halim, A.; Nilsson, J.; Rüetschi, U.; Hesse, C.; Larson, G. *Mol. Cell. Proteomics* **2012**, *11* (4), 013649.
(25) Tajiri, M.; Yoshida, S.; Wada, Y. *Glycobiology* **2005**, *15* (12), 1332−1340.
(26) Hwang, H.; Lee, J. Y.; Lee, H. K.; Park, G. W.; Jeong, H. K.; Moon, M. H.; Kim, J. Y.; Yoo, J. S. *Anal. Bioanal. Chem.* **2014**, *406* (30), 7999−8011.
(27) Clerc, F.; Reiding, K. R.; Jansen, B. C.; Kammeijer, G. S. M.; Bondt, A.; Wuhrer, M. *Glycoconjugate J.* **2016**, *33* (3), 309−343.
(28) Spicer, V.; Yamchuk, A.; Cortens, J.; Sousa, S.; Ens, W.; Standing, K. G.; Wilkins, J. A.; Krokhin, O. V. *Anal. Chem.* **2007**, *79* (22), 8762−8768.
(29) Hanstein, A.; Muller-Eberhard, U. *Journal of Laboratory and Clinical Medicine* **1968**, *71* (2), 232−239.
(30) Nilsson, S. C.; Sim, R. B.; Lea, S. M.; Fremeaux-Bacchi, V.; Blom, A. M. *Mol. Immunol.* **2011**, *48* (14), 1611−1620.
(31) Noris, M.; Remuzzi, G. *Semin. Nephrol.* **2013**, *33* (6), 479−492.
(32) Kasperska-Zajac, A.; Grzanka, A.; Machura, E.; Misiolek, M.; Mazur, B.; Jochem, J. *J. Inflammation (London, U. K.)* **2013**, *10*, 22−22.
(33) Ogedegbe, H. O.; Brown, D. W. *Lab. Med.* **2001**, *32* (7), 384−389.
(34) He, Q.-Y.; Yang, H.; Wong, B. C.; Chiu, J.-F. *Dig. Dis. Sci.* **2008**, *53* (12), 3112.

DOI: 10.1021/acs.analchem.9b00776
Anal. Chem. 2019, 91, 5433−5445